

## FEED-FORWARD NETWORKS, CENTER MANIFOLDS, AND FORCING

MARTIN GOLUBITSKY

Mathematical Biosciences Institute  
The Ohio State University  
Columbus, OH 43215, USA

CLAIRE POSTLETHWAITE

Department of Mathematics  
University of Auckland  
Auckland 1142, New Zealand

**ABSTRACT.** This paper discusses feed-forward chains near points of synchrony-breaking Hopf bifurcation. We show that at synchrony-breaking bifurcations the center manifold inherits a feed-forward structure and use this structure to provide a simplified proof of the theorem of Elmhirst and Golubitsky that there is a branch of periodic solutions in such bifurcations whose amplitudes grow at the rate of  $\lambda^{\frac{1}{6}}$ . We also use this center manifold structure to provide a method for classifying the bifurcation diagrams of the forced feed-forward chain where the amplitudes of the periodic responses are plotted as a function of the forcing frequency. The bifurcation diagrams depend on the amplitude of the forcing, the deviation of the system from Hopf bifurcation, and the ratio  $\gamma$  of the imaginary part of the cubic term in the normal form of Hopf bifurcation to the real part. These calculations generalize the results of Zhang on the forcing of systems near Hopf bifurcations to three-cell feed-forward chains.

**1. Introduction.** This paper discusses several aspects of feed-forward chains near points of synchrony-breaking bifurcations. Specifically, we consider the three-cell feed-forward chain shown in Figure 1, the equations of which can be written as

$$\begin{aligned}\dot{x}_1 &= f(x_1, x_1, \lambda) \\ \dot{x}_2 &= f(x_2, x_1, \lambda) \\ \dot{x}_3 &= f(x_3, x_2, \lambda)\end{aligned}\tag{1}$$

where  $x_1, x_2, x_3 \in \mathbf{R}^m$  and  $\lambda \in \mathbf{R}$  is a bifurcation parameter. We examine the dynamics near Hopf bifurcation of both this system and additionally of the same system under the influence of a small amplitude sinusoidal forcing.



FIGURE 1. Three-cell feed-forward network

---

2000 *Mathematics Subject Classification.* Primary: 34C25; Secondary: 37G15.

*Key words and phrases.* Center manifolds, feed-forward networks, Hopf bifurcation.

This system has been considered in previous work first by [5], who observed that the amplitude of periodic solutions grows at the surprising rate of  $\lambda^{\frac{1}{6}}$ , rather than the expected rate of  $\lambda^{\frac{1}{2}}$ . They also observed in simulations that the branch was stable. The existence of this branch in a generic synchrony-breaking Hopf bifurcation was proved by Elmhirst and Golubitsky [3] using Liapunov-Schmidt methods. In this paper, we are able to reproduce this result in a much simpler fashion, by considering the center manifold of the system and using normal form techniques. Our methods also allow us to prove that these solutions are stable when they are supercritical.

The periodic forcing of systems near Hopf bifurcation has been well studied (see Gambaudo [4] and the introduction to [11]). Zhang [10, 11] showed that three small-amplitude periodic solutions were possible in the forcing of systems near a point of Hopf bifurcation and classified the various ways multiplicity can occur. In this paper, we also extend the results of Zhang by considering the existence of small amplitude periodic solutions of a small amplitude sinusoidally-forced three-cell feed-forward chain. We show that multiplicity of up to five solutions is possible near a point of synchrony-breaking Hopf bifurcation and classify the ways that multiplicity can occur.

*Review of synchrony-breaking Hopf bifurcation.* We assume that (1) has a supercritical synchrony-breaking Hopf bifurcation at the origin. Specifically:

- We assume there is a synchronous equilibrium, which WLOG is at the origin; that is,  $f(0, 0, \lambda) = 0$ .
- The Jacobian for system (1) at the origin has the form

$$J = \begin{pmatrix} a+b & 0 & 0 \\ b & a & 0 \\ 0 & b & a \end{pmatrix} \quad (2)$$

where  $a = f_1(0)$  and  $b = f_2(0)$ , the subscripts refer to partial derivatives, and 0 denotes 0, 0, 0. It follows from (2) that the eigenvalues of  $J$  are the eigenvalues of the  $m \times m$  matrices  $a+b$  and  $a$  with the eigenvalues of  $a$  repeated twice. For ease of discussion we assume that the eigenvalues of  $a+b$  have negative real part so that locally solutions to the first equation in (1) tend to  $x_1 = 0$ .

- Synchrony-breaking bifurcations occur when the eigenvalues of  $a$  are critical. We assume that the synchronous equilibrium is stable when  $\lambda < 0$  and at  $\lambda = 0$  the matrix  $a$  has a pair of simple pure imaginary eigenvalues.
- We assume that there is only one independent eigenvector of  $J$  associated to the critical eigenvalue of  $a$ , which is a nondegeneracy assumption on the matrix  $b$ .
- Therefore, the equation  $\dot{x} = f(x, 0, \lambda)$  undergoes a Hopf bifurcation at  $\lambda = 0$ , which we assume is supercritical.

It follows that the second equation  $\dot{x}_2 = f(x_2, 0, \lambda)$  undergoes a standard Hopf bifurcation at  $\lambda = 0$ . The assumption that this Hopf bifurcation is supercritical implies generically the existence of a unique family of periodic trajectories  $x_2^\lambda(t)$  for  $\lambda > 0$  whose amplitudes grow at the rate of  $\lambda^{\frac{1}{2}}$ . The third equation in (1) now has the form

$$\dot{x}_3 = f(x_3, x_2^\lambda(t), \lambda); \quad (3)$$

of a system near Hopf bifurcation that is periodically forced by a function whose frequency is near the Hopf frequency. This 1:1 resonance is caused by the fact

that the eigenvalues of  $a$  are forced by network architecture to be double. So, as discussed in [3], the  $\lambda^{\frac{1}{6}}$  growth rate of small amplitude periodic solutions  $x_3^\lambda(t)$  to (3) is due to resonance.

*Review of periodic forcing of systems near Hopf bifurcation.* The issue that is most often addressed in such small-amplitude forced systems is: How do the periodic solutions of the forced system having the same frequency as the frequency of the forcing vary with the forcing frequency? This problem is complicated by having three small parameters: the deviation of the unforced system from Hopf bifurcation  $\lambda$ , the small amplitude  $\varepsilon$  of the forcing, and the deviation of the forcing frequency from the Hopf frequency  $\omega = 1 - \omega_F$ . It is known that for many systems such as the forced Duffing equation (see Bogoliubov and Mitropolsky [1]) there is a range of forcing frequencies with multiple periodic responses. This behavior is captured in the full truncated normal form:

$$f(z_2, z_1, \lambda) = (\lambda + i - (1 + \gamma i)|z_1|^2)z_1 + z_2 \quad (4)$$

where  $\gamma \in \mathbf{R}$ . In [6] it is shown that multiplicity occurs for  $\lambda < 0$  when  $\gamma > \sqrt{3}$  but not otherwise. In her thesis Zhang [10] (see [11]) gives a complete description of the bifurcation diagrams obtained by plotting the amplitude of the periodic solutions as a function of the forcing frequency  $\omega$ . These diagrams depend on two small parameters  $\lambda$  and  $\varepsilon$ ; qualitatively, there are five different possible bifurcation diagrams, which are included in the cell 2 diagrams in this paper. See Figures 5 and 7.

*Review of the forced feed-forward chain near Hopf bifurcation.* The forced feed-forward chain was previously considered by McCullen *et al.* [9]. They showed that periodically forcing feed-forward chains near points of Hopf bifurcation can lead to sensitive bandwidth filters. More precisely, they assumed that the  $f$  in (1) is in truncated normal form for Hopf bifurcation with linear coupling; that is,

$$f(z_2, z_1, \lambda) = (\lambda + i - |z_2|^2)z_2 + z_1 \quad (5)$$

where  $z_1, z_2 \in \mathbf{C}$ . They then assumed that the chain was forced by small-amplitude periodic forcing in the first node by replacing the self-coupling by sinusoidal forcing; that is

$$\dot{z}_1 = (\lambda + i - |z_1|^2)z_1 + \varepsilon e^{i\omega_F t} \quad (6)$$

where  $\omega_F \approx 1$  is the forcing frequency.

McCullen *et al.* [9] also explored the forced feed-forward chain both numerically and experimentally when  $\lambda < 0$  is subcritical; that is, when the trivial equilibrium is still (weakly) stable. Note that when  $\lambda < 0$  the solution to the first forced equation in (1) (that is, equation (6)) when  $\varepsilon$  is sufficiently small is periodic with amplitude of order  $\varepsilon$ . It follows that the second equation in (1) is just an equation near Hopf bifurcation that is being forced by small amplitude periodic solutions.

*Main results.* In section 2 we consider center manifolds of synchrony-breaking bifurcations in feed-forward chains and show that the dynamics on the center manifold also has the structure of a feed-forward chain (Theorem 2.3). This result applies to any synchrony-breaking bifurcation in the chain. In section 3 we consider specifically a synchrony-breaking Hopf bifurcation of a feed-forward chain. We show that the truncated Birkhoff normal form can be assumed to be  $\mathbf{S}^1$ -equivariant (Theorem 3.1), as is the case for the standard Hopf bifurcation, allowing us to recover

the  $\lambda^{\frac{1}{6}}$  growth rate result (Theorem 3.3). The proof of normal form is deferred to Appendix A.

In the last sections of the paper we classify the bifurcation diagrams of amplitude of response versus forcing frequency in both cells 2 and 3. This is accomplished by first showing in section 4 that the periodic forcing of a system near criticality is qualitatively the same as the periodic forcing of the center manifold equations (Lemma 4.1).

Lemma 4.1 allows us to study the bifurcation on the center manifold in section 5. This study is accomplished by using the  $\mathbf{S}^1$ -equivariance of the forced system to see that in rotating coordinates periodic solutions become equilibria. Bifurcation diagrams are then distinguished by computing (with a combination of analysis and numerics) the singularity theory bifurcation and hysteresis varieties in both cells 2 and 3. We do not attempt to prove that the results are independent of terms of order greater than 3 in the truncated normal form, though we believe that they are. We also do not attempt to determine the stability of the periodic solutions that we find. The calculations in [11] show just how complicated such a calculation may be expected to be.

**2. Center manifold of feed-forward system.** We consider the three-cell feed-forward system shown in figure 1. Equations for this system can be written as in (1). As noted in the Introduction we assume that  $a+b$  has eigenvalues with negative real part, so  $x_1 \rightarrow 0$ . We thus ignore the first cell and consider the system

$$\begin{aligned} (a) \quad \dot{x}_2 &= f(x_2, 0) \\ (b) \quad \dot{x}_3 &= f(x_3, x_2) \end{aligned} \tag{7}$$

where we have dropped the dependence of  $f$  on  $\lambda$  for convenience. The linearization about 0 is then

$$J = \begin{pmatrix} a & 0 \\ b & a \end{pmatrix}$$

We will now show that the flow restricted to the center manifold of (7) has the same feedforward structure. This is proved in Theorem 2.3, but first we need two lemmas.

**Lemma 2.1.** *The flow of (7) can be written*

$$\Phi_t(x_2, x_3) = (\phi_t(x_2, 0), \phi_t(x_3, x_2))$$

*Proof.* The feed forward structure of (7) implies that its flow has the form

$$\Phi_t(x_2, x_3) = (\hat{\phi}_t(x_2), \phi_t(x_3, x_2))$$

where

$$\left. \frac{d\hat{\phi}_t}{dt}(x_2) \right|_{t=0} = f(x_2, 0) \quad \text{and} \quad \left. \frac{d\phi_t}{dt}(x_3, x_2) \right|_{t=0} = f(x_3, x_2).$$

Therefore,

$$\left. \frac{d\phi_t}{dt}(x_3, 0) \right|_{t=0} = f(x_3, 0) = \left. \frac{d\hat{\phi}_t}{dt}(x_3) \right|_{t=0}. \tag{8}$$

Since (8) holds for all  $x_3$ , it follows that

$$\frac{d\hat{\phi}_t}{dt}(x_3) = \frac{d\phi_t}{dt}(x_3, 0)$$

Thus  $\hat{\phi}_t(x_3) = \phi_t(x_3, 0)$  and  $\hat{\phi}_t(x_2) = \phi_t(x_2, 0)$ .  $\square$

We assume that the center subspace of  $a$  is the dimension  $n$  subspace  $\mathbf{E}^c$ . It follows that the center subspace of (7) is the  $2n$ -dimensional subspace  $\mathbf{E}^c \oplus \mathbf{E}^c$ . Let  $\pi_2(x_2, x_3) = (x_2, 0)$  be the projection onto the first coordinate of  $\mathbf{R}^m \times \mathbf{R}^m$ .

Let  $\mathcal{V}^c \times \{0\}$  be a  $n$ -dimensional center manifold of (7)(a) in  $\mathbf{R}^m \times \{0\}$ . It follows from Lemma 2.1 and the fact that  $\mathcal{V}^c \times \{0\}$  is flow-invariant for (7)(a) that  $\pi_2^{-1}(\mathcal{V}^c \times \{0\}) = \mathcal{V}^c \times \mathbf{R}^m$  is flow-invariant for (7). Therefore, we can choose a  $2n$ -dimensional center manifold  $\mathcal{W}^c$  for (7) in  $\pi_2^{-1}(\mathcal{V}^c \times \{0\})$  and

$$\pi_2(\mathcal{W}^c) = \mathcal{V}^c \times \{0\}. \tag{9}$$

Note that  $\{0\} \times \mathcal{V}^c$  is flow invariant for (7). More precisely, (7)(a) has 0 as a fixed-point and (7)(b) on  $x_2 = 0$  is exactly the same equation as (7)(a). We can choose  $\mathcal{W}^c$  so that

$$\{0\} \times \mathcal{V}^c \subset \mathcal{W}^c \tag{10}$$

is a submanifold. This would follow directly if center manifolds were unique since  $\mathcal{W}^c \cap (\{0\} \times \mathbf{R}^k)$  would also be a center manifold with center subspace  $\{0\} \times E^c$ . However, center manifolds are unique once a cutoff function is chosen (see Carr [2]) and we can chose a cutoff function for  $\mathcal{W}^c$  that is equal for  $\{0\} \times \mathcal{V}^c$  and  $\mathcal{V}^c \times \{0\}$ .

**Lemma 2.2.** *The manifold  $\mathcal{V}^c \times \{0\}$  is a submanifold of  $\mathcal{W}^c$  and  $\mathcal{W}^c$  is a fiber bundle over the base  $\mathcal{V}^c \times \{0\}$  with fibers isomorphic to  $\{0\} \times \mathcal{V}^c$ .*

*Proof.* First, we show that

$$\mathcal{V}^c \times \{0\} \subset \mathcal{W}^c \tag{11}$$

We prove (11) by verifying that

$$\mathcal{V}^c \times \{0\} = \mathcal{W}^c \cap (\mathbf{R}^m \times \{0\}).$$

To verify this claim, define

$$\hat{\mathcal{V}}^c = \mathcal{W}^c \cap (\mathbf{R}^m \times \{0\}).$$

and note that  $\hat{\mathcal{V}}^c$  is a  $n$ -dimensional manifold. Also note that  $\pi_2$  is the identity on  $\mathbf{R}^m \times \{0\}$  and hence  $\pi_2(\hat{\mathcal{V}}^c) = \hat{\mathcal{V}}^c$ . Therefore,

$$\hat{\mathcal{V}}^c = \pi_2(\hat{\mathcal{V}}^c) = \pi_2(\mathcal{W}^c \cap (\mathbf{R}^m \times \{0\})).$$

Since  $\pi_2(A \cap B) \subset \pi_2(A) \cap \pi_2(B)$  for any  $A, B$ , it follows using (9) that

$$\begin{aligned} \hat{\mathcal{V}}^c &\subset \pi_2(\mathcal{W}^c) \cap \pi_2(\mathbf{R}^m \times \{0\}) \\ &= (\mathcal{V}^c \times \{0\}) \cap (\mathbf{R}^m \times \{0\}) \\ &= \mathcal{V}^c \times \{0\} \end{aligned}$$

Since  $\mathcal{V}^c \times \{0\}$  and  $\hat{\mathcal{V}}^c$  are manifolds of the same dimension, it follows that  $\hat{\mathcal{V}}^c = \mathcal{V}^c \times \{0\}$ , thus verifying the claim.

Second, choose coordinates  $(z_2, 0)$  and  $(0, z_3)$  on  $\mathcal{V}^c \times \{0\}$  and  $\{0\} \times \mathcal{V}^c$  respectively. We write  $\mathcal{W}^c$  as a fiber bundle with base  $\mathcal{V}^c \times \{0\}$ . For each  $z_2$ , define the fiber over  $z_2$  as

$$\mathcal{U}_{z_2} = \mathcal{W}^c \cap (\{z_2\} \times \mathbf{R}^m) = \{z \in \mathcal{W}^c : \pi_2(z) = z_2\}.$$

Note that  $\mathcal{U}_0 = \{0\} \times \mathcal{V}^c$ . □

Since  $\mathcal{W}^c$  is a fiber bundle, for each  $z_2$  there exists a mapping

$$\rho : (z_2, \{0\} \times \mathcal{V}^c) \rightarrow \mathcal{U}_{z_2},$$

so  $\rho(z_2, z_3) \in \mathcal{U}_{z_2}$ . This mapping satisfies  $\rho(0, z_3) = z_3$  (since  $\mathcal{U}_0 = \{0\} \times \mathcal{V}^c$ ) and  $\rho(z_2, 0) = 0$  (since the base is preserved).

**Theorem 2.3.** *The dynamics on the center manifold  $\mathcal{W}^c$  of (7) can be written on  $\mathcal{V}^c \times \mathcal{V}^c$  as*

$$\begin{aligned}\dot{z}_2 &= g(z_2, 0) \\ \dot{z}_3 &= g(z_3, z_2)\end{aligned}$$

for some function  $g$  and coordinates  $z_2, z_3 \in \mathcal{V}^c$ .

**Remark 1.** In previous work [5] we did not see how to prove that the  $\dot{z}_2$  equation could be taken to be  $g(z_2, 0)$ . The improvement here is based on the center manifold construction in Lemma 2.2. In other networks where a nilpotent Hopf bifurcation occurs this conclusion is not valid. See Remark 2.

*Proof.* We coordinatize the flow on  $\mathcal{W}^c$  with a mapping  $P : \mathcal{V}^c \times \mathcal{V}^c \rightarrow \mathcal{W}^c$  defined by

$$P(z_2, z_3) = (z_2, \rho(z_2, z_3)).$$

with  $\rho(0, z_3) = z_3$ .  $P$  is invertible and the inverse has the form

$$P^{-1}(z_2, z_3) = (z_2, \sigma(z_2, z_3))$$

where  $\sigma$  satisfies

$$\sigma(z_2, \rho(z_2, z_3)) = z_3$$

and in particular

$$\sigma(0, \rho(0, z_3)) = \sigma(0, z_3) = z_3$$

Denote the flow on  $\mathcal{V}^c \times \mathcal{V}^c$  by  $\Psi_t(z_2, z_3)$ . Then

$$\begin{aligned}\Psi_t(z_2, z_3) &= P^{-1}\Phi_t P(z_2, z_3) \\ &= P^{-1}\Phi_t(z_2, \rho(z_2, z_3)) \\ &= P^{-1}(\phi_t(z_2, 0), \phi_t(\rho(z_2, z_3), z_2)) \\ &= (\phi_t(z_2, 0), \sigma(\phi_t(z_2, 0), \phi_t(\rho(z_2, z_3), z_2)))\end{aligned}$$

Write the second coordinate of  $\Psi_t(z_2, z_3)$  as  $\psi_t(z_3, z_2)$  and compute

$$\begin{aligned}\psi_t(z_3, 0) &= \sigma(\phi_t(0, 0), \phi_t(\rho(0, z_3), 0)) \\ &= \sigma(0, \phi_t(z_3, 0)) \\ &= \phi_t(z_3, 0)\end{aligned}$$

Thus  $\phi_t(z_2, 0) = \psi_t(z_2, 0)$  and we can write the flow on  $\mathcal{V}^c \times \mathcal{V}^c$  as

$$\psi_t(z_2, z_3) = (\psi_t(z_2, 0), \psi_t(z_3, z_2)),$$

which implies that the differential equations can be written as stated.  $\square$

**Remark 2.** There are other feed-forward networks that have nilpotent double eigenvalues that lead via Hopf bifurcations to equations of the form

$$\begin{aligned}\dot{x}_2 &= g(x_2, \lambda) \\ \dot{x}_3 &= h(x_3, x_2, \lambda)\end{aligned}\tag{12}$$

where  $g(0, \lambda) = 0 = h(0, 0, \lambda)$  and  $dg$  and  $d_{x_3}h$  have the same matrix  $a(\lambda)$  at the equilibrium  $x_2 = x_3 = 0$ . This situation occurs in the network shown in

Figure 2. In this case the two center manifolds  $\mathcal{V}_1^c \times \{0\}$  and  $\{0\} \times \mathcal{V}_2^c$  cannot be naturally identified and the vector fields on these center manifolds cannot be naturally identified. For example the Hopf bifurcation of the equation on the first center manifold might be supercritical and on the second subcritical, which can happen in the network in Figure 2. Nevertheless the results described here are still valid; the center manifold for the feed-forward system is a fiber bundle parametrized by  $\mathcal{V}_1^c \times \mathcal{V}_2^c$  and the center manifold equations have the same form as (12); that is,

$$\begin{aligned} \dot{z}_2 &= \hat{g}(z_2, \lambda) \\ \dot{z}_3 &= \hat{h}(z_3, z_2, \lambda) \end{aligned} \tag{13}$$

where  $z_2, z_3 \in \mathbf{C}$  and  $\hat{g}(0, 0) = \hat{h}(0, 0, 0) = i$ .

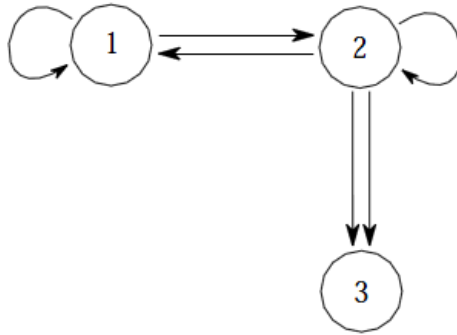


FIGURE 2. Three-cell feed-forward network with antiphase periodic solution.

**Remark 3.** The center manifold arguments resulting in Theorem 2.3 (as well as the normal form arguments in the next section summarized in Theorem 3.1) can be iterated to apply to feed-forward chains of arbitrary length. A theorem about the form of center manifolds in general feed-forward networks should be possible.

**3. Hopf bifurcation normal form and solutions.** The previous section discussed the form of the center manifold equations on a feed-forward network and was applicable to any type of bifurcation. We now concentrate on Hopf bifurcation. That is, we assume the center subspace  $\mathbf{E}^c$  in cell 2 is two-dimensional, and the linearization of the internal dynamics  $a$  has a pair of purely imaginary eigenvalues at  $\lambda = 0$ . We rescale time so these are equal to  $\pm i$ . Theorem 2.3 showed that on the center manifold, the dynamics are given by

$$\begin{aligned} \dot{z}_2 &= g(z_2, 0), \\ \dot{z}_3 &= g(z_3, z_2). \end{aligned} \tag{14}$$

for coordinates  $z_2, z_3 \in \mathbf{C}$ . Theorem 3.1 shows that we can transform (14) into Birkhoff normal form such that the resulting system is  $\mathbf{S}^1$  equivariant and Theorem 3.3 uses this equivariance to prove the existence of a branch of  $\lambda^{\frac{1}{6}}$  growth rate solutions.

**Theorem 3.1.** *For any value of  $k$ , there exists a polynomial change of coordinates which can transform (14) into the form*

$$\begin{aligned}\dot{z}_2 &= p_k(z_2) + \cdots \\ \dot{z}_3 &= p_k(z_3) + q_k(z_3, z_2) + \cdots\end{aligned}\tag{15}$$

where  $p_k$  and  $q_k$  are polynomials of order  $k$ ,  $q_k(z_3, 0) = 0$ , and  $\cdots$  indicates terms of degree at least  $k + 1$ . The truncated system

$$\begin{aligned}\dot{z}_2 &= p_k(z_2) \\ \dot{z}_3 &= p_k(z_3) + q_k(z_3, z_2)\end{aligned}\tag{16}$$

is equivariant under the action of  $\mathbf{S}^1$  given by

$$\theta(z_2, z_3) = (e^{i\theta} z_2, e^{i\theta} z_3)$$

Theorem 3.1 is proved using standard procedures of Birkhoff normal form theory; the proof is contained in Appendix A.

**Remark 4.** Putting the center manifold equations (13) for the network in figure 2 into normal form works identically to the proof of Theorem 3.1 and those normal form equations also have  $\mathbf{S}^1$ -equivariance.

After rescaling time so that the Hopf frequency is 1 and explicitly including the bifurcation parameter  $\lambda$ , the  $\mathbf{S}^1$ -equivariant normal form equations have the form

$$\begin{aligned}\dot{z}_2 &= \hat{p}(|z_2|^2, \lambda) z_2 \\ \dot{z}_3 &= \hat{p}(|z_3|^2, \lambda) z_3 + \hat{q}(z_2, z_3, \lambda)\end{aligned}\tag{17}$$

where  $z_2, z_3 \in \mathbf{C}$ ,  $\hat{p}, \hat{q} \in \mathbf{C}$ , and

$$\begin{aligned}\hat{p}(0, 0) &= i \\ \hat{q}(0, z_3, \lambda) &= 0 \\ \hat{q}(e^{i\theta} z_2, e^{i\theta} z_3, \lambda) &= e^{i\theta} \hat{q}(z_2, z_3, \lambda)\end{aligned}\tag{18}$$

Because of the  $\mathbf{S}^1$ -equivariance, periodic solutions will be rotating waves with frequency near 1. That is, we can assume

$$\begin{aligned}z_2 &= e^{i(1+\tau)t} u_2 \\ z_3 &= e^{i(1+\tau)t} u_3\end{aligned}\tag{19}$$

where  $\tau \approx 0$  and  $u_2, u_3 \in \mathbf{C}$ . Substituting (19) into (17) yields

$$\begin{aligned}\dot{u}_2 &= (\hat{p}(|u_2|^2, \lambda) - (1 + \tau)i) u_2 \\ \dot{u}_3 &= (\hat{p}(|u_3|^2, \lambda) - (1 + \tau)i) u_3 + \hat{q}(u_2, u_3, \lambda)\end{aligned}\tag{20}$$

Observe that steady-state solutions to (20) correspond to rotating waves periodic solutions of (17). Moreover, if we set  $p = \hat{p} - i$ , then we need to solve the equations

$$\begin{aligned}0 &= (p(|u_2|^2, \lambda) - \tau i) u_2 \\ 0 &= (p(|u_3|^2, \lambda) - \tau i) u_3 + \hat{q}(u_2, u_3, \lambda)\end{aligned}\tag{21}$$

where  $p \in \mathbf{C}$  and  $p(0, 0) = 0$ .

The first equation in (21) is just the equation that is solved in standard Hopf bifurcation. We assume that the Hopf bifurcation in cell 2 is supercritical where the equilibrium is stable for  $\lambda < 0$ . Begin by writing  $p = p^R + ip^I$ . It follows that

$$\tau = p^I(|u_2|^2, \lambda)$$

Next, we assume the *eigenvalue crossing condition* and the *Hopf condition*

$$p_\lambda^R(0, 0) > 0 \quad \text{and} \quad p_u^R(0, 0) < 0\tag{22}$$

where  $u = |u_2|^2$ . We can use  $\mathbf{S}^1$ -equivariance to assume  $u_2 \geq 0$ . It follows by the implicit function theorem applied to  $p^R = 0$  that there is a unique branch of solutions to  $p^R(u_2^2, \lambda) = 0$ . Moreover, that solution grows in amplitude at the rate of  $\sqrt{\lambda}$ . Specifically,

$$u_2^2(\lambda) = \lambda r(\lambda)$$

where

$$r(0) = -\frac{p_\lambda^R(0, 0)}{p_u^R(0, 0)} > 0.$$

It follows that

$$u_2(\lambda) = \lambda^{\frac{1}{2}} s(\lambda) \tag{23}$$

where  $s(\lambda) = \sqrt{r(\lambda)}$  and  $s(0) > 0$ .

To solve the second equation in (21) we must be more explicit about the form of  $\hat{q}$ .

**Lemma 3.2.** *Let  $\hat{q}(z_2, z_3, \lambda)$  satisfy the  $\mathbf{S}^1$ -equivariance condition in (18). Then*

$$\hat{q}(z_2, z_3) = A(|z_2|^2, |z_3|^2, z_2\bar{z}_3, \lambda)z_2 + B(|z_2|^2, |z_3|^2, \bar{z}_2z_3, \lambda)z_3 \tag{24}$$

where  $A, B \in \mathbf{C}$  are unique and

$$B(0, |z_3|^2, 0, \lambda) = 0. \tag{25}$$

*Proof.* It is known that the quadratic polynomials

$$|z_2|^2 \quad |z_3|^2 \quad z_2\bar{z}_3 \quad \bar{z}_2z_3$$

form a Hilbert basis for the  $\mathbf{S}^1$ -invariant functions of  $\mathbf{C} \times \mathbf{C} \rightarrow \mathbf{C}$  and that  $z_2, z_3$  are generators for the  $\mathbf{S}^1$ -equivariant mappings of  $\mathbf{C} \times \mathbf{C} \rightarrow \mathbf{C}$  over the ring of  $\mathbf{S}^1$ -invariant functions. Thus we can write

$$\hat{q}(z_2, z_3) = A(|z_2|^2, |z_3|^2, z_2\bar{z}_3, \bar{z}_2z_3, \lambda)z_2 + B(|z_2|^2, |z_3|^2, \bar{z}_2z_3, z_2\bar{z}_3, \lambda)z_3$$

for some functions  $A, B \in \mathbf{C}$ . Note that

$$(\bar{z}_2z_3)z_2 = |z_2|^2z_3 \quad \text{and} \quad (z_2\bar{z}_3)z_3 = |z_3|^2z_2.$$

It follows that we can assume that  $A$  is independent of the Hilbert generator  $\bar{z}_2z_3$  and that  $B$  is independent of the Hilbert generator  $z_2\bar{z}_3$ . No further reductions are possible. So  $\hat{q}$  has the form (24). Also note that

$$\hat{q}(0, z_3, \lambda) = B(0, |z_3|^2, 0, \lambda)z_3$$

so that (25) follows from (18). □

We can use (25) to further specify the form of  $B$ . Specifically, we claim that

$$B(|z_2|^2, |z_3|^2, \bar{z}_2z_3, \lambda) = C(|z_2|^2, |z_3|^2, \bar{z}_2z_3, \lambda)|z_2|^2 + D(|z_2|^2, |z_3|^2, \bar{z}_2z_3, \lambda)\bar{z}_2z_3 \tag{26}$$

To verify (26) note that (25) implies that each nonzero monomial in  $B$  has either a  $|z_2|^2$  factor or a  $\bar{z}_2z_3$  factor.

We can now summarize that the form of the second equation in (21) must be:

$$0 = (p^R(|u_3|^2, \lambda) + i(p^I(|u_3|^2, \lambda) - p^I(u_2^2, \lambda)))u_3 + A(u_2^2, |u_3|^2, u_2\bar{u}_3, \lambda)u_2 + C(u_2^2, |u_3|^2, u_2u_3, \lambda)u_2^2u_3 + D(u_2^2, |u_3|^2, u_2u_3, \lambda)u_2u_3^2 \tag{27}$$

where  $p^R(0) = p^I(0) = 0$  and  $u_2 = \lambda^{\frac{1}{2}}s(\lambda) \geq 0$ .

**Theorem 3.3.** *There exists a unique branch of stable solutions  $u_3(\lambda)$  to (27) and that branch has a growth rate of  $\lambda^{\frac{1}{6}}$ .*

*Proof.* Assume that the solution has the form  $u_3(\mu)$  where  $\mu^\kappa = \lambda$ , for some  $\kappa$ . Then to lowest order,  $u_3(\mu)$  is of order  $\mu$ , and we can expand (27) in powers of  $\mu$  as follows

$$0 = (p^R(\mu^2, \mu^\kappa) + i(p^I(\mu^2, \mu^\kappa) - p^I(\mu^\kappa, \mu^\kappa))) \mu + A(\mu^\kappa, \mu^2, \mu^{\frac{\kappa}{2}+1}, \mu^\kappa) \mu^{\frac{\kappa}{2}} + C(\mu^\kappa, \mu^2, \mu^{\frac{\kappa}{2}+1}, \mu^\kappa) \mu^{\kappa+1} + D(\mu^\kappa, \mu^2, \mu^{\frac{\kappa}{2}+1}, \mu^\kappa) \mu^{\frac{\kappa}{2}+2}$$

The lowest orders are 3 and  $\frac{\kappa}{2}$ . These orders can balance only when  $\kappa = 6$ . When  $\kappa = 6$  we see that

$$0 = (p^R(\mu^2, \mu^6) + i(p^I(\mu^2, \mu^6) - p^I(\mu^6, \mu^6))) \mu + A(\mu^6, \mu^2, \mu^4, \mu^6) \mu^3 + C(\mu^6, \mu^2, \mu^4, \mu^6) \mu^7 + D(\mu^6, \mu^2, \mu^4, \mu^6) \mu^5 \tag{28}$$

Write  $u_3 = \mu y$  and  $u_2 = \mu^3 s(\mu^6)$ . We now write (27) modulo terms of order  $\mu^6$  and obtain

$$p(\mu^2|y|^2, 0)\mu y + A(0, \mu^2|y|^2, 0, 0)\mu^3 s + D(0)\mu^5 s y^2 = 0 \tag{29}$$

where  $D(0) = D(0, 0, 0, 0)$ . Using Taylor series and dividing by  $\mu^3$ , we can simplify (29) as

$$\Sigma(y, \mu) = p_u(0)|y|^2 y + A(0)s + \left( \frac{1}{2} p_{uu}(0)|y|^4 y + A_v(0)|y|^2 s + D(0) s y^2 \right) \mu^2 + O(\mu^4)$$

where  $A(0) = A(0, 0, 0, 0)$ . Note that  $\Sigma(y, 0) = 0$  can be solved for  $y_0$  as follows:

$$\Sigma(y, 0) = p_u(0)|y|^2 y + A(0)s(0) = 0$$

Specifically,

$$|y|^2 y = -\frac{A(0)}{p_u(0)} s(0) = -\frac{A(0)}{p_u(0)} \sqrt{-\frac{p_\lambda^R(0)}{p_u^R(0)}}$$

If we write

$$-\frac{A(0)}{p_u(0)} = \hat{R} e^{i\varphi}$$

then the unique solution will be given by  $Re^{i\varphi}$  where

$$R^3 = \hat{R} \sqrt{-\frac{p_\lambda^R(0)}{p_u^R(0)}}$$

It follows that  $y_0 = Re^{i\varphi}$ .

We can now apply the implicit function theorem to solve  $\Sigma(y, \mu) = 0$  for  $y = y(\mu^2)$ . The determinant of the Jacobian  $D\Sigma(y_0, 0)$  is obtained by computing  $|\Sigma_y(y_0, 0)|^2 - |\Sigma_{\bar{y}}(y_0, 0)|^2$ . We compute

$$\Sigma_y = 2p_u(0)|y|^2 \quad \text{and} \quad \Sigma_{\bar{y}} = p_u(0)y^2$$

Therefore

$$\det(D\Sigma)_{y_0,0} = 3|p_u(0)|^2|y_0|^4 = 3|p_u(0)|^2 R^4 > 0 \tag{30}$$

Finally, we compute the stability of the solutions  $(u_2(\lambda), u_3(\lambda))$ . Note that we need to determine four Floquet exponents. Since the  $\dot{u}_2$  equation is decoupled we can conclude that one exponent is 1 and due to exchange of stability one has negative real part. The other two Floquet exponents are determined by the  $\dot{u}_3$

equation. Since the periodic solutions are rotating waves we need only determine the stability of the equilibrium to (21). To do this we compute the signs of the real parts of the eigenvalues of  $D\Sigma$ . We show that these signs are negative at the origin (since we were able to divide by  $\mu^3$ ) and hence by continuity they are negative along the branch. We have already computed the determinant in (30), so we need only compute the trace at the origin. It is

$$\text{tr}(D\Sigma)_{y_0,0} = 2\text{Re}(\Sigma_y(y_0, 0)) = 4\text{Re}(p_u(0)|y_0|^2) = 4p_u^R(0)R^2 < 0$$

Since the determinant is positive and the trace is negative, the solution is stable.  $\square$

**Remark 5.** We continue the discussion about the network in figure 2 given in Remarks 2 and 4. If both solution branches are supercritical, then we can use the same arguments as in Theorem 3.3 we can show the existence of a branch of solutions whose amplitude growth of  $\lambda^{\frac{1}{6}}$ .

**4. Center manifold of forced systems.** Consider the system

$$\dot{x} = f(x, \lambda) + \varepsilon g(t) \tag{31}$$

where the unforced system

$$\dot{x} = f(x, \lambda) \tag{32}$$

is such that  $f(0, \lambda) = 0$  and  $Df(0, 0)$  has a center subspace  $\mathbf{E}^c$ . All other eigenvalues of  $Df(0, 0)$  have negative real part. Equation (32) has an attracting center manifold  $\mathcal{W}^c$  which is tangent to  $\mathbf{E}^c$  at  $(0, 0)$ .

**Lemma 4.1.** *Let  $x(t)$  be a small amplitude bounded solution to (31). Then  $\{x(t)\} \subset \mathcal{W}^c$ .*

*Proof.* The unforced equation can be decomposed into the flow on  $\mathcal{W}^c$ , and the flow transverse to  $\mathcal{W}^c$ . The flow transverse is contracting onto  $\mathcal{W}^c$ , and on a bounded neighborhood of the origin the rate of contraction has a minimum which is bounded away from zero.

Consider the bounded trajectory  $x(t)$  for (31), and consider the rate of contraction onto  $\mathcal{W}^c$  over the closure of that trajectory. Let  $-\mu^c(x)$  be the rate at which points on the trajectory converge to the center manifold and let  $\mu^e(x)$  be the rate at which due to forcing the solution is driven away from the center manifold. Note that  $\mu^e(x)$  depends on the amplitude  $\varepsilon$  of the forcing. Let  $\mu_{\min} = \min \mu^c(x) > 0$ . We can always choose  $\varepsilon$  small enough so that the minimum contraction  $\mu_{\min}$  onto  $\mathcal{W}^c$  is greater than the maximum expansion due to the forcing. Therefore, the trajectory  $x(t)$  must lie inside of  $\mathcal{W}^c$ .  $\square$

**5. Solution branches in forced chains.** In this section we consider a feedforward chain with small amplitude forcing, and compute the branches of periodic solutions with the same frequency as the forcing for a specific example. We do not prove that the results for the example we consider are generic, although we believe that they are.

The equilibrium in cell 1 is stable, and so small amplitude forcing of cell 1 will produce a small amplitude periodic solution. For simplicity, we ignore this step, and simply replace the coupling from cell 1 to cell 2 of the feedforward chain with small amplitude periodic forcing of cell 2. We consider additive forcing, so we can apply

lemma 4.1 and need only consider forcing the center manifold. By theorems 2.3 and 3.1 the normal form of the unforced system can be written in the form

$$\begin{aligned}\dot{z}_2 &= \hat{p}(|z_2|^2, \lambda)z_2 \\ \dot{z}_3 &= \hat{p}(|z_3|^2, \lambda)z_3 + \hat{q}(z_2, z_3, \lambda)\end{aligned}$$

For ease of calculation we consider a cubic truncation of the internal dynamics, and a linear truncation of the forcing term, and take a single sinusoidal forcing term, that is, we consider the equations (after appropriate rescaling):

$$\begin{aligned}\dot{z}_2 &= (\lambda + i)z_2 + (-1 + i\gamma)|z_2|^2z_2 + \varepsilon e^{i\omega_F t}, \\ \dot{z}_3 &= (\lambda + i)z_3 + (-1 + i\gamma)|z_3|^2z_3 + z_2\end{aligned}$$

We do not attempt to prove that the results are independent of terms of higher order, neither do we compute the stability of solutions.

To begin, we change to rotating coordinates, that is, we write

$$z_j = u_j e^{i(\omega_F t - \theta_j)}, \quad j = 1, 2$$

to obtain

$$\begin{aligned}\dot{u}_2 &= (\lambda + i\omega)u_2 + (-1 + i\gamma)|u_2|^2u_2 - \varepsilon e^{i\theta_1} \\ \dot{u}_3 &= (\lambda + i\omega)u_3 + (-1 + i\gamma)|u_3|^2u_3 - u_2 e^{i(\theta_2 - \theta_1)}\end{aligned}$$

where  $\omega = 1 - \omega_F$ . We set  $\dot{u}_j = 0$  and solve

$$\begin{aligned}g(u_2) &\equiv (\lambda + i\omega)u_2 + (-1 + i\gamma)|u_2|^2u_2 = \varepsilon e^{i\theta_1} \\ g(u_3) &= -u_2 e^{i(\theta_2 - \theta_1)}\end{aligned}$$

which is equivalent to

$$\begin{aligned}|g(u_2)|^2 &= \varepsilon^2 \\ |g(u_3)|^2 &= |u_2|^2\end{aligned}$$

where

$$|g(u)|^2 = (\lambda^2 + \omega^2)|u|^2 + 2(\omega\gamma - \lambda)|u|^4 + (1 + \gamma^2)|u|^6.$$

Set  $\delta = \varepsilon^2$  and  $R_j = |u_j|^2$  and let

$$G(R; \lambda, \omega, \gamma) \equiv (1 + \gamma^2)R^3 + 2(\omega\gamma - \lambda)R^2 + (\lambda^2 + \omega^2)R$$

For solutions, we have to solve

$$G(R_2; \lambda, \omega, \gamma) = \delta \tag{33}$$

$$G(R_3; \lambda, \omega, \gamma) = R_2 \tag{34}$$

We consider  $R_2, R_3$  as a function of  $\omega$  for fixed  $\lambda, \gamma, \delta$ . In order to construct bifurcation diagrams we find curves of hysteresis points and bifurcation points for fixed  $\gamma$  in  $\lambda$ - $\delta$  space.

**5.1. Results from a single cell.** We recap the results for a single forced cell, that is, solutions  $R_2$  of (33). These calculations are described in detail in [10, 11] and are based on the singularity theory construction of hysteresis and bifurcation varieties, as described in [7, Chapter III, §5]. These varieties divide parameter space into regions of qualitatively similar bifurcation diagrams. Parameter values where bifurcation diagrams have vertical tangents are called *hysteresis points* and parameter values where bifurcation diagrams are not smooth curves (such as when bifurcation diagrams contain crossed branches) are called *bifurcation points*. More

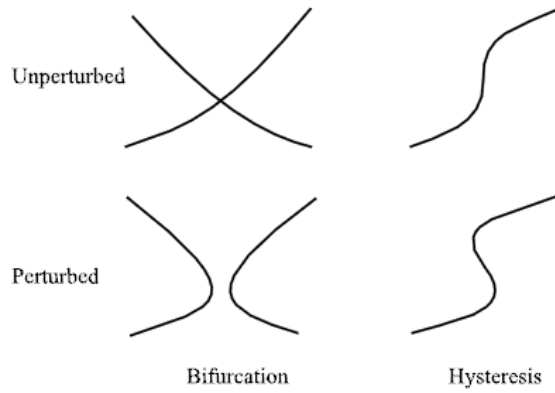


FIGURE 3. Bifurcation and hysteresis phenomena. Adapted from [7, Chapter III, §5].

specifically,  $S$ -shaped curves that lead to multiplicity of solutions are formed at hysteresis points. New components (such as the spawning of an isola) and the rearranging of components (such as happens at perturbations of transcritical bifurcations) occur at bifurcation points. In Figure 3 we show sketches of solutions at points of bifurcation and hysteresis, along with solutions after a small perturbation.

5.1.1. *Hysteresis points.* Hysteresis points are found by solving

$$G(R_2; \lambda, \omega, \gamma) = \delta \tag{35}$$

$$G_R(R_2; \lambda, \omega, \gamma) = 0 \tag{36}$$

$$G_{RR}(R_2; \lambda, \omega, \gamma) = 0 \tag{37}$$

(plus some more conditions on various derivatives being non-zero). It can be shown that in  $\delta$ - $\lambda$  space there are two hysteresis curves at:

$$\lambda = \left( \frac{\sqrt{3}}{2} \frac{\sqrt{3} - \gamma}{(1 + \gamma^2)^{1/3}} \right) \delta^{1/3}$$

$$\lambda = \left( \frac{\sqrt{3}}{2} \frac{\sqrt{3} + \gamma}{(1 + \gamma^2)^{1/3}} \right) \delta^{1/3}$$

Note that if  $\gamma < \sqrt{3}$  then the coefficient of  $\delta^{1/3}$  in both of these equations is positive. If  $\gamma > \sqrt{3}$  then the first is negative, and the second is positive.

As part of the calculation, we also find (which is useful in the following) that at hysteresis points, the following conditions are also satisfied:

$$(\omega\gamma - \lambda) = -\frac{3}{2}(1 + \gamma^2)^{2/3}\delta^{1/3} \tag{38}$$

$$(\lambda^2 + \omega^2) = 3(1 + \gamma^2)^{1/3}\delta^{2/3} \tag{39}$$

5.1.2. *Bifurcation points.* Bifurcation points are found by solving

$$G(R_2; \lambda, \omega, \gamma) = \delta$$

$$G_R(R_2; \lambda, \omega, \gamma) = 0$$

$$G_\omega(R_2; \lambda, \omega, \gamma) = 0$$

There are two curves of bifurcation points in  $\delta$ - $\lambda$  space. The first is given by  $\delta = 0$  for  $\lambda > 0$ . The second bifurcation curve occurs at

$$\lambda = \frac{3}{2^{2/3}} \delta^{1/3}$$

**5.2. Results for third cell.** We now compute the solutions  $R_3$  in the third cell. We suppose that the equation  $G(R_2; \lambda, \omega, \gamma) = \delta$  has been solved in the second cell, then we can think of the input  $R_2$  into the third cell as a function  $R_2(\lambda, \omega, \gamma, \delta)$ . The equation for  $R_3$  in the third cell is thus:

$$G(R_3; \lambda, \omega, \gamma) = R_2(\lambda, \omega, \gamma, \delta).$$

We again proceed by computing curves of hysteresis and bifurcation points in  $\delta$ - $\lambda$  space.

**5.2.1. Hysteresis points.** Hysteresis points occur when

$$G(R_2; \lambda, \omega, \gamma) = \delta \tag{40}$$

$$G(R_3; \lambda, \omega, \gamma) = R_2 \tag{41}$$

$$G_R(R_3; \lambda, \omega, \gamma) = 0 \tag{42}$$

$$G_{RR}(R_3; \lambda, \omega, \gamma) = 0 \tag{43}$$

Equations (41) to (43) are equivalent to equations (35) to (37), with  $\delta$  and  $R_2$  replaced by  $R_2$  and  $R_3$  respectively. Thus we have already solved these, and we can substitute these solutions into (40). That is, we have

$$(1 + \gamma^2)R_2^3 + 2(\omega\gamma - \lambda)R_2^2 + (\lambda^2 + \omega^2)R_2 = \delta \tag{44}$$

where

$$(\omega\gamma - \lambda) = -\frac{3}{2}(1 + \gamma^2)^{2/3}R_2^{1/3} \tag{45}$$

$$(\lambda^2 + \omega^2) = 3(1 + \gamma^2)^{1/3}R_2^{2/3} \tag{46}$$

(from (38) and (39)) and  $R_2$  is given by

$$\lambda = \left( \frac{\sqrt{3}}{2} \frac{\sqrt{3} \pm \gamma}{(1 + \gamma^2)^{1/3}} \right) R_2^{1/3} \tag{47}$$

Substituting (45) and (46) into (44) gives

$$(1 + \gamma^2)R_2^3 - 3(1 + \gamma^2)^{2/3}R_2^{7/3} + 3(1 + \gamma^2)^{1/3}R_2^{5/3} = \delta \tag{48}$$

At leading order, we only need the final term on the left hand side, that is

$$3(1 + \gamma^2)^{1/3}R_2^{5/3} = \delta$$

substituting for  $R_2$  from (47) gives

$$\frac{2^5}{3^{3/2}} \frac{(1 + \gamma^2)^2}{(\sqrt{3} \pm \gamma)^5} \lambda^5 = \delta$$

that is,

$$\lambda = \frac{3^{3/10}}{2} \frac{(\sqrt{3} \pm \gamma)}{(1 + \gamma^2)^{2/5}} \delta^{1/5} \tag{49}$$

So this gives two additional curves of hysteresis points. If  $\gamma < \sqrt{3}$ , both have positive coefficient, that is, both curves lie in the right-hand side of the  $\lambda$ - $\delta$  plane.

If  $\gamma > \sqrt{3}$ , one has positive coefficient and one negative, so there is one curve in the right-hand side and one in the left-hand side of the  $\lambda$ - $\delta$  plane.

5.2.2. *Bifurcation points.* Bifurcation points occur when

$$G(R_2; \lambda, \omega, \gamma) = \delta \quad (50)$$

$$G(R_3; \lambda, \omega, \gamma) = R_2 \quad (51)$$

$$G_R(R_3; \lambda, \omega, \gamma) = 0 \quad (52)$$

$$G_\omega(R_3; \lambda, \omega, \gamma) + R_2 \omega(\lambda, \omega, \gamma, \delta) = 0 \quad (53)$$

Equation (53) can also be written as

$$G_\omega(R_3; \lambda, \omega, \gamma) + \frac{G_\omega(R_2; \lambda, \omega, \gamma)}{G_R(R_2; \lambda, \omega, \gamma)} = 0$$

We assume that in the limit of small  $\lambda$ , solutions to these equations are of the form

$$\delta = \hat{\delta} \lambda^{\alpha_\delta}, \quad R_2 = \hat{R}_2 \lambda^{\alpha_{R_2}}, \quad R_3 = \hat{R}_3 \lambda^{\alpha_{R_3}}, \quad \omega = \hat{\omega} \lambda^{\alpha_\omega}$$

This leads to the following set of equations:

$$\begin{aligned} (1 + \gamma^2) \hat{R}_2^3 \lambda^{3\alpha_{R_2}} + 2\gamma \hat{\omega} \hat{R}_2^2 \lambda^{2\alpha_{R_2} + \alpha_\omega} - 2\hat{R}_2^2 \lambda^{2\alpha_{R_2} + 1} + \hat{R}_2 \lambda^{\alpha_{R_2} + 2} \\ + \hat{\omega}^2 \hat{R}_2 \lambda^{\alpha_{R_2} + 2\alpha_\omega} = \hat{\delta} \lambda^{\alpha_\delta} \\ (1 + \gamma^2) \hat{R}_3^3 \lambda^{3\alpha_{R_3}} + 2\gamma \hat{\omega} \hat{R}_3^2 \lambda^{2\alpha_{R_3} + \alpha_\omega} - 2\hat{R}_3^2 \lambda^{2\alpha_{R_3} + 1} + \hat{R}_3 \lambda^{\alpha_{R_3} + 2} \\ + \hat{\omega}^2 \hat{R}_3 \lambda^{\alpha_{R_3} + 2\alpha_\omega} = \hat{R}_2 \lambda^{\alpha_{R_2}} \\ 3(1 + \gamma^2) \hat{R}_3^2 \lambda^{2\alpha_{R_3}} + 4\gamma \hat{\omega} \hat{R}_3 \lambda^{\alpha_{R_3} + \alpha_\omega} - 4\hat{R}_3 \lambda^{\alpha_{R_3} + 1} + \hat{\omega}^2 \lambda^{2\alpha_\omega} + \lambda^2 = 0 \\ (\gamma \hat{R}_3^2 \lambda^{2\alpha_{R_3}} + \hat{\omega} \hat{R}_3 \lambda^{\alpha_{R_3} + \alpha_\omega})(3(1 + \gamma^2) \hat{R}_2^2 \lambda^{2\alpha_{R_2}} + 4\gamma \hat{\omega} \hat{R}_2 \lambda^{\alpha_{R_2} + \alpha_\omega} \\ - 4\hat{R}_2 \lambda^{\alpha_{R_2} + 1} + \hat{\omega}^2 \lambda^{2\alpha_\omega} + \lambda^2) + (\gamma \hat{R}_2^2 \lambda^{2\alpha_{R_2}} + \hat{\omega} \hat{R}_2 \lambda^{\alpha_{R_2} + \alpha_\omega}) = 0 \end{aligned}$$

One possible scaling is

$$\alpha_\delta = 5, \quad \alpha_{R_2} = 3, \quad \alpha_{R_3} = 1, \quad \alpha_\omega = 1$$

At leading order, the equations become (dropping the hats)

$$R_2(1 + \omega^2) = \delta \quad (54)$$

$$(1 + \gamma^2)R_3^3 + 2(\omega\gamma - 1)R_3^2 + (1 + \omega^2)R_3 = R_2 \quad (55)$$

$$3(1 + \gamma^2)R_3^2 + 4(\gamma\omega - 1)R_3 + (\omega^2 + 1) = 0 \quad (56)$$

$$(\gamma R_3^2 + \omega R_3)(1 + \omega^2) = -\omega R_2 \quad (57)$$

Eliminating  $R_2$  from (57) and (55) gives

$$(1 + \gamma^2)R_3^3 + \left(2(\omega\gamma - 1) + \frac{\gamma}{\omega}(1 + \omega^2)\right)R_3^2 + 2(1 + \omega^2)R_3 = 0 \quad (58)$$

which simplifies to become

$$(1 + \gamma^2)R_3^2 + \left(\frac{3\omega^2\gamma - 2\omega + \gamma}{\omega}\right)R_3 + 2(1 + \omega^2) = 0 \quad (59)$$

Eliminating  $R_3^2$  from (56) and (59) gives

$$R_3 = \frac{-5\omega(1 + \omega^2)}{2\omega(\omega\gamma - 1) + 3\gamma(1 + \omega^2)} \quad (60)$$

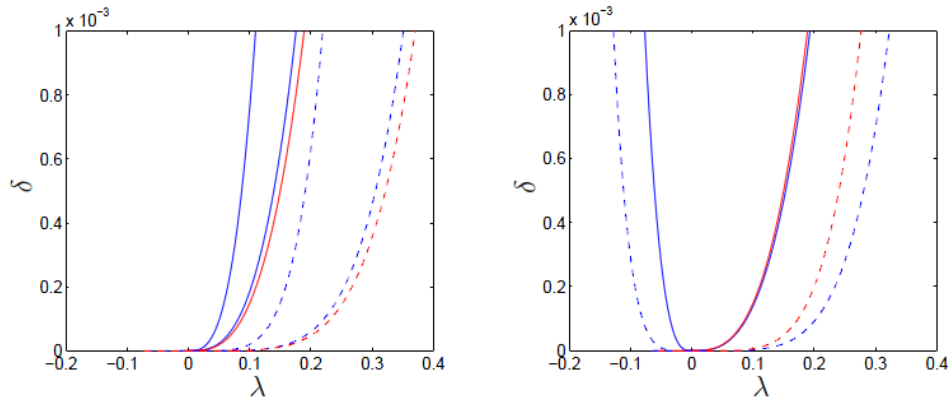


FIGURE 4. The figures show bifurcation and hysteresis curves in  $\lambda$ - $\delta$  space for  $\gamma = 0.4 < \gamma^*$  (left) and  $\gamma = 4 > \sqrt{3}$  (right). The values of  $\gamma$  used for computation were far from  $\gamma^*$  and  $\sqrt{3}$  so that the individual curves can be easily distinguished in the figure. For  $\gamma^* < \gamma < \sqrt{3}$  the picture is the same as the left hand figure except that the right most red and blue dashed curves are the other way around. We do not show this figure as the curves would be too close to distinguish. Solid curves represent bifurcations/hysteresis in both cells, dashed curves are just for cell 2. Blue curves are hysteresis curves, red curves are bifurcation curves. The six curves divide the plane into seven regions each of which has a different bifurcation diagram when solutions are plotted for  $R_j$  against  $\omega$ . These diagrams are shown in Figures 5, 6 and 7.

Substituting for  $R_3$  in (56) gives an equation for  $\omega$  implicitly in terms of  $\gamma$ . After simplification we find

$$(\omega + \gamma)(25\omega^3 + 15\gamma\omega^2 + 13\omega + 3\gamma) = 0 \quad (61)$$

The solution with  $\omega = -\gamma$  corresponds to the solution  $\delta = 0$  which was previously computed. It can be shown that the cubic bracket has only one real root, regardless of the value of  $\gamma$ . The cubic can be solved numerically for  $\omega$  as a function of  $\gamma$ , which then gives  $R_3$ ,  $R_2$  and  $\delta$  as functions of  $\gamma$  using (60), (57) and (54). Numerical simulations show that this bifurcation curve is in the right-half of the  $\lambda$ - $\delta$  plane. Numerical solutions also show there is some  $\gamma^* \approx 1.15$  such that the bifurcation curve lies below both hysteresis curves if  $\gamma < \gamma^*$ , and above the right-hand hysteresis curve if  $\gamma > \gamma^*$ .

**5.3. Schematic pictures.** We plot the resulting bifurcation and hysteresis curves for fixed  $\gamma$  in  $\lambda$ - $\delta$  space, showing examples in Figure 4. The curves are plotted numerically so that we can show the numerical solution of the bifurcation curves for cell 3. Note that because the hysteresis and bifurcation curves for cell 2 have  $\delta \sim \lambda^3$  these lie above (for small enough  $\lambda$ ) the hysteresis and bifurcation curves for cell 3, which have  $\delta \sim \lambda^5$ . The curves are thus shown in the limit of small  $\lambda$ . The six curves divide the plane into seven regions.

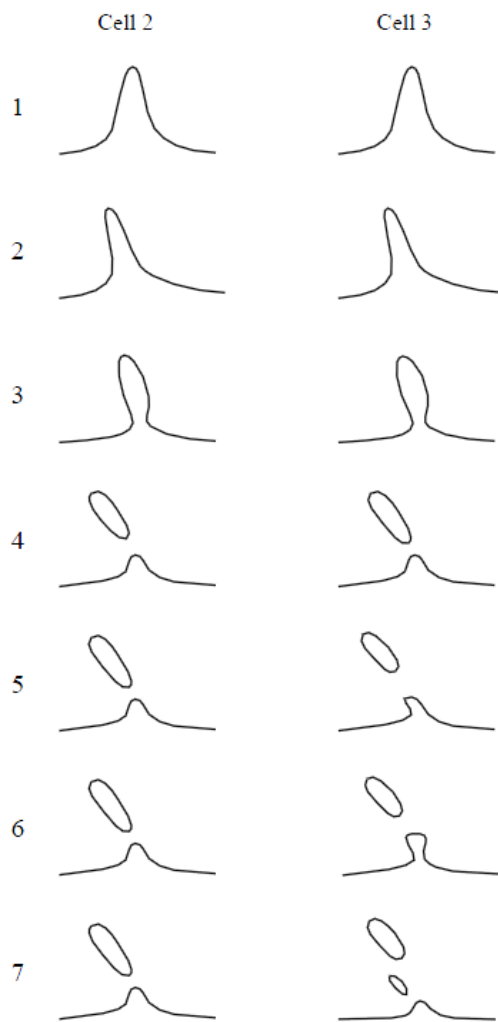


FIGURE 5. Each subfigure shows a schematic of a bifurcation diagram for each of the seven regions of the  $\delta$ - $\lambda$  plane, for  $\gamma < \gamma^*$ . In each subfigure,  $R_j$  is plotted against  $\omega$ , for  $j = 2$  (cell 2, left column) and  $j = 3$  (cell 3, right column). The seven regions are shown in Figure 4, and the numbers label the regions from left to right.

For each of the seven regions, we show schematic plots of amplitude of solution against  $\omega$  in each cell are sketched schematically in Figures 5, 6 and 7. Notice that there is the possibility of multiplicity of up to five solutions in cell 3.

**Appendix A. Proof of Theorem 3.1.** This appendix contains the proof of Theorem 3.1. Recall that Theorem 2.3 showed that on the center manifold, the dynamics

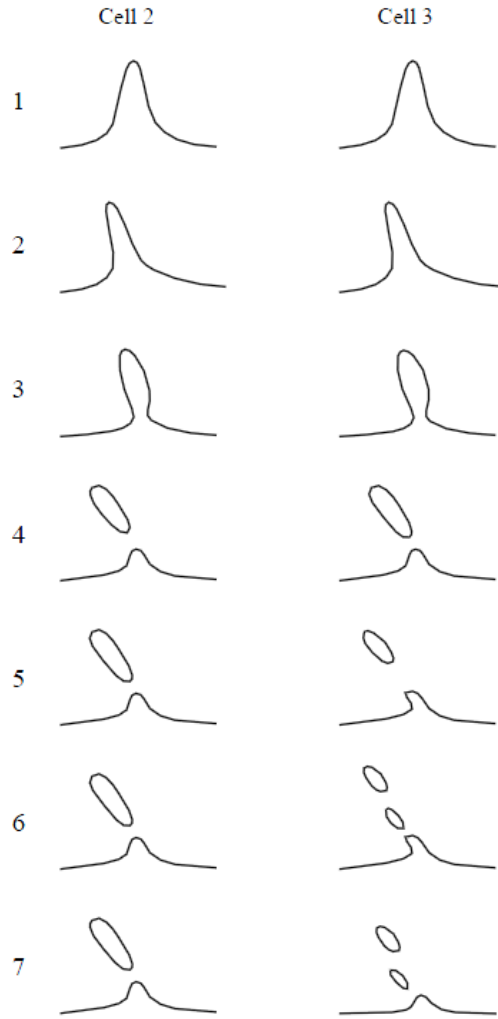


FIGURE 6. Each subfigure shows a schematic of a bifurcation diagram for each of the seven regions of the  $\delta$ - $\lambda$  plane, for  $\gamma^* < \gamma < \sqrt{3}$ . In each subfigure,  $R_j$  is plotted against  $\omega$ , for  $j = 2$  (cell 2, left column) and  $j = 3$  (cell 3, right column). The numbers label the regions from left to right in the  $\delta$ - $\lambda$  plane.

are given by

$$\begin{aligned} \dot{z}_2 &= g(z_2, 0), \\ \dot{z}_3 &= g(z_3, z_2). \end{aligned} \tag{A.1}$$

for coordinates  $z_2, z_3 \in \mathbf{C}$ . We now show that we can perform a series of near-identity transformations to put the system into Birkhoff normal form such that the resulting system is  $\mathbf{S}^1$  equivariant.

It is clear that transformations of the form

$$\begin{pmatrix} z_2 \\ z_3 \end{pmatrix} \rightarrow \begin{pmatrix} p_1(z_2) \\ p_1(z_3) \end{pmatrix}$$

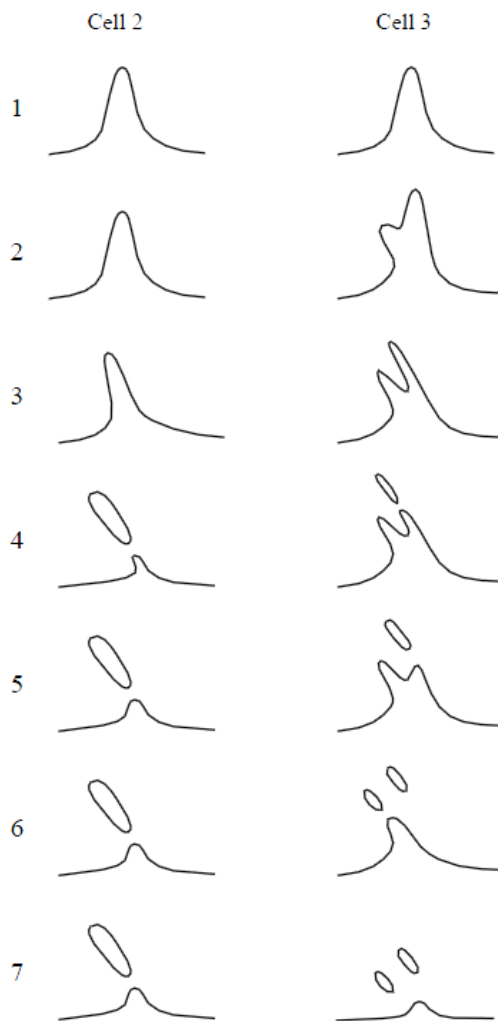


FIGURE 7. Each subfigure shows a schematic of a bifurcation diagram for each of the seven regions of the  $\delta$ - $\lambda$  plane, for  $\gamma > \sqrt{3}$ . In each subfigure,  $R_j$  is plotted against  $\omega$ , for  $j = 2$  (cell 2, left column) and  $j = 3$  (cell 3, right column). The seven regions are shown in Figure 4, and the numbers label the regions from left to right.

do not change the structure of equations (A.1). Since the first equation in (A.1) is independent of  $z_3$ , we can thus make transformations of this type (following the standard Birkhoff normal form transformations for Hopf bifurcation) so that the first equation is in the standard Hopf normal form. We assume these transformations have already been done up to some order  $k \in \mathbf{N}$ , that is, we can write  $g(z_2, 0) = p(z_2) + \dots$ , where  $p(z_2) = \bar{p}(|z_2|^2)z_2$  and  $\dots$  refer to terms of order greater than  $k$ .

The following lemma shows that we can make coordinate changes only to the  $z_3$  coordinate and preserve the structure of the equations.

**Lemma A.1.** *Let  $\Phi_t(z_2, z_3)$  be the flow for (A.1) and let  $P$  be a near identity change of coordinates of the form*

$$P(z_2, z_3) = (z_2, \rho(z_3, z_2))$$

where  $\rho(z_3, 0) = z_3$ . Then the flow  $\Psi_t = P^{-1}\Phi_t P$  is also associated to a system in the form (A.1).

*Proof.* It follows from the assumption that  $\Phi_t(z_2, z_3)$  is the flow of (A.1) that  $\Phi_t$  has the form

$$\Phi_t(z_2, z_3) = (\phi_t(z_2, 0), \phi_t(z_3, z_2))$$

To verify the lemma we must show that  $\Psi_t$  has the form

$$\Psi_t(z_2, z_3) = (\psi_t(z_2, 0), \psi_t(z_3, z_2)) \tag{A.2}$$

To verify (A.2) compute

$$\Psi_t(z_2, z_3) = P^{-1}\Phi_t(z_2, \rho(z_3, z_2)) = P^{-1}(\phi_t(z_2, 0), \phi_t(\rho(z_3, z_2), z_2))$$

Since  $P$  maps the plane  $(z_2, \cdot)$  it follows that  $P^{-1}$  must also. Therefore,  $P^{-1}(z_2, z_3) = (z_2, \sigma(z_3, z_2))$  where

$$\sigma(\rho(z_3, z_2), z_2) = z_3$$

To see this compute

$$P^{-1}P(z_2, z_3) = P^{-1}(z_2, \rho(z_3, z_2)) = (z_2, \sigma(\rho(z_3, z_2), z_2))$$

Hence

$$\Psi_t(z_2, z_3) = (\phi_t(z_2, 0), \sigma(\phi_t(\rho(z_3, z_2), z_2), \phi_t(z_2, 0))) \tag{A.3}$$

Suppose

$$\Psi_t(z_2, z_3) = (a_t(z_2, z_3), b_t(z_3, z_2)).$$

It follows from (A.3) that  $a_t$  is independent of  $z_3$  and  $a_t(z_2) = \phi_t(z_2, 0)$ . It also follows that

$$b_t(z_3, 0) = \sigma(\phi_t(\rho(z_3, 0), 0), 0) = \sigma(\phi_t(z_3, 0), 0) = \phi_t(z_3, 0) = a_t(z_3)$$

as needed. □

In the proof of Theorem 3.1 we use coordinate changes of the type described in Lemma A.1 to transform the center manifold equations into Birkhoff normal form.

*Proof of Theorem 3.1.* First, write  $g(z_2, 0) = h(z_2)$ . Then this implies that we can write  $g(z_3, z_2) = h(z_3) + \hat{h}(z_3, z_2)$  where  $\hat{h}(z_3, 0) = 0$ . We have assumed that we have already made coordinate transformations so that  $h(z_2) = p_k(z_2) + \dots$ , where  $p_k$  is an order- $k$   $\mathbf{S}^1$ -equivariant polynomial, that is  $p_k(z_2) = \tilde{p}_k(|z_2|^2)z_2$ .

We now seek to find a further series of near-identity transformations of the form

$$\begin{pmatrix} z_2 \\ z_3 \end{pmatrix} \rightarrow \begin{pmatrix} z_2 \\ z_3 + P_k(z_2, z_3) \end{pmatrix} \tag{A.4}$$

where  $P_k$  is a polynomial of order  $k$ , and  $P_k(0, z_3) = 0$ , to transform the equations into the desired form. We follow the standard procedure of Birkhoff normal form theory (see [8] for more details).

Proceeding by induction, we make a succession of coordinate changes to eliminate terms of successive orders. We thus assume that  $g(z_2, z_3)$  has the form

$$g(z_2, z_3) = f_k(z_2, z_3) + h_k(z_2, z_3) + \dots$$

where  $f_k$  consists of terms up to order  $k - 1$  which cannot be removed, and  $h_k$  are terms of order  $k$ . The linear part of (A.1) is

$$L = \begin{pmatrix} \alpha & 0 \\ \beta & \alpha \end{pmatrix}$$

where  $\alpha(z_2) = iz_2$  and  $\beta(z_2) = \beta_1 z_2 + \beta_2 \bar{z}_2$ . Let  $\mathcal{P}_k$  be the space of homogeneous polynomial mappings of degrees  $k$  on  $\mathbf{C}^2$  which satisfy  $P_k(0, z_3) = 0$  for each  $P_k \in \mathcal{P}_k$ . Let  $P_k \in \mathcal{P}_k$  and write

$$\tilde{P}_k = \begin{pmatrix} 0 \\ P_k(z_2, z_3) \end{pmatrix}$$

Then computation of the adjoint of  $\tilde{P}_k$ , defined below, allows us to compute which terms can be removed by coordinate transformations of the form given in (A.4). The adjoint is defined as:

$$\text{ad}_L(\tilde{P}_k)(z) = L\tilde{P}_k(z) - (d\tilde{P}_k)_z Lz$$

where  $z = (z_2, z_3)^T$ , and  $(d\tilde{P}_k)_{z_2}(z_2) = (d\tilde{P}_k)_{z_2} z_2 + (d\tilde{P}_k)_{\bar{z}_2} \bar{z}_2$ . Computing, we find (dropping the dependence of  $P_k$  on  $z_2$  and  $z_3$  for clarity):

$$\begin{aligned} \text{ad}_L(\tilde{P}_k)(z) &= L\tilde{P}_k(z) - (d\tilde{P}_k)_z Lz \\ &= \begin{pmatrix} \alpha & 0 \\ \beta & \alpha \end{pmatrix} \begin{pmatrix} 0 \\ P_k \end{pmatrix} - \begin{pmatrix} 0 & 0 \\ dP_{kz_2} & dP_{kz_3} \end{pmatrix} \begin{pmatrix} \alpha & 0 \\ \beta & \alpha \end{pmatrix} \begin{pmatrix} z_2 \\ z_3 \end{pmatrix} \\ &= \begin{pmatrix} 0 \\ iP_k \end{pmatrix} - \begin{pmatrix} 0 & 0 \\ dP_{kz_2} & dP_{kz_3} \end{pmatrix} \begin{pmatrix} iz_2 \\ iz_3 + \beta_1 z_2 + \beta_2 \bar{z}_2 \end{pmatrix} \\ &= \begin{pmatrix} 0 \\ \mathcal{A}(P_k) \end{pmatrix} \end{aligned}$$

where

$$\begin{aligned} \mathcal{A}(P_k) &= i(P_k - dP_{kz_2} z_2 + dP_{k\bar{z}_2} \bar{z}_2 - dP_{kz_3} z_3 + dP_{k\bar{z}_3} \bar{z}_3) \\ &\quad - (\beta_1 dP_{kz_3} z_2 + \beta_2 dP_{kz_3} \bar{z}_2 + \bar{\beta}_1 dP_{k\bar{z}_3} \bar{z}_2 + \bar{\beta}_2 dP_{k\bar{z}_3} z_2) \end{aligned} \tag{A.5}$$

Note that  $\mathcal{A}(P_k)(0, z_3) = 0$ , so  $\mathcal{A}(P_k)$  is a linear map  $\mathcal{P}_k \rightarrow \mathcal{P}_k$ . The terms which can be eliminated from the center manifold equations by the transformation (A.4) are those in the subspace  $\mathcal{A}(\mathcal{P}_k) \subset \mathcal{P}_k$ .

We now find the form of all possible terms of polynomials in  $\mathcal{A}(\mathcal{P}_k)$ . Consider  $Q_k \in \mathcal{P}_k$ , where  $Q_k = z_2^{\alpha_1} \bar{z}_2^{\alpha_2} z_3^{\alpha_3} \bar{z}_3^{\alpha_4}$ , for  $\alpha_j \in \mathbf{N}$ . We will show that  $Q_k \in \mathcal{A}(\mathcal{P}_k)$  so long as  $(1 - \alpha_1 + \alpha_2 - \alpha_3 + \alpha_4) \neq 0$ . Note that  $Q_k(0, z_3) = 0$  implies that at least one of  $\alpha_1$  and  $\alpha_2$  are greater than zero. We also assume here that  $\beta_1 \beta_2 \neq 0$  but the other cases can be dealt with similarly.

Write  $\hat{\alpha} = (1 - \alpha_1 + \alpha_2 - \alpha_3 + \alpha_4)$  and assume  $\hat{\alpha} \neq 0$ . We compute

$$\begin{aligned} \mathcal{A}(Q_k) &= i(1 - \alpha_1 + \alpha_2 - \alpha_3 + \alpha_4) z_2^{\alpha_1} \bar{z}_2^{\alpha_2} z_3^{\alpha_3} \bar{z}_3^{\alpha_4} \\ &\quad - (\beta_1 \alpha_3 z_2^{\alpha_1+1} \bar{z}_2^{\alpha_2} z_3^{\alpha_3-1} \bar{z}_3^{\alpha_4} + \bar{\beta}_1 \alpha_4 z_2^{\alpha_1} \bar{z}_2^{\alpha_2+1} z_3^{\alpha_3} \bar{z}_3^{\alpha_4-1} \\ &\quad + \beta_2 \alpha_3 z_2^{\alpha_1} \bar{z}_2^{\alpha_2+1} z_3^{\alpha_3-1} \bar{z}_3^{\alpha_4} + \bar{\beta}_2 \alpha_4 z_2^{\alpha_1+1} \bar{z}_2^{\alpha_2} z_3^{\alpha_3} \bar{z}_3^{\alpha_4-1}) \end{aligned} \tag{A.6}$$

First consider the case  $\alpha_3 = \alpha_4 = 0$ . Then

$$\mathcal{A} \left( \frac{Q_k}{i\hat{\alpha}} \right) = Q_k$$

so we immediately see that  $Q_k \in \mathcal{A}(\mathcal{P}_k)$ .

Next consider the case  $\alpha_3 \neq 0$ ,  $\alpha_4 = 0$ . We proceed by induction on  $\alpha_3$ . Assume that for  $\alpha_3 > 1$  we have found  $q_{13}, q_{23}$  such that

$$\begin{aligned}\mathcal{A}(q_{13}) &= z_2^{\alpha_1+1} \bar{z}_2^{\alpha_2} z_3^{\alpha_3-1} \\ \mathcal{A}(q_{23}) &= z_2^{\alpha_1} \bar{z}_2^{\alpha_2+1} z_3^{\alpha_3-1}\end{aligned}$$

Then

$$\mathcal{A}\left(\frac{1}{i\hat{\alpha}}\left(Q_k + \frac{1}{\beta_1\alpha_3}q_{13} + \frac{1}{\beta_2\alpha_3}q_{23}\right)\right) = Q_k$$

so  $Q_k \in \mathcal{A}(\mathcal{P}_k)$ . For the first step in the induction process, that is, for  $\alpha_3 = 1$ , we have  $q_{13} = \frac{1}{i\hat{\alpha}} z_2^{\alpha_1+1} \bar{z}_2^{\alpha_2}$  and  $q_{14} = \frac{1}{i\hat{\alpha}} z_2^{\alpha_1} \bar{z}_2^{\alpha_2+1}$ . Similar computations by induction also apply for the cases  $\alpha_4 \neq 0$ ,  $\alpha_3 = 0$  and  $\alpha_3, \alpha_4 \neq 0$ .

Therefore the only terms which cannot be removed are those for which  $(1 - \alpha_1 + \alpha_2 - \alpha_3 + \alpha_4) = 0$ . These terms are precisely those of the form

$$h_2(|z_2|^2, |z_3|^2, z_2 \bar{z}_3, z_3 \bar{z}_2) z_2 \quad \text{or} \quad h_3(|z_2|^2, |z_3|^2, z_2 \bar{z}_3, z_3 \bar{z}_2) z_3$$

for polynomials  $h_1, h_2$ , that is, terms which are equivariant with respect to the action of  $\mathbf{S}^1$ . □

**Acknowledgments.** We thank Ian Stewart for many helpful conversations specifically concerning Remarks 2, 4, and 5. This research was supported in part by NSF Grant DMS-1008412 to MG, a University of Auckland Research Committee Grant to CMP, the Mathematical Biosciences Institute (NSF Grant DMS-0931642), and the New Zealand Institute for Mathematics and its Applications.

#### REFERENCES

- [1] N. N. Bogoliubov and Y. A. Mitropolsky, “Asymptotic Methods in the Theory of Non-linear Oscillations,” Translated from the second revised Russian edition, International Monographs on Advanced Mathematics and Physics, Hindustan Publ. Corp., Delhi, Gordon and Breach Science Publishers, New York, 1961.
- [2] J. Carr, “Applications of Centre Manifold Theory,” Applied Mathematical Sciences, **35**, Springer-Verlag, New York-Berlin, 1981.
- [3] T. Elmhirst and M. Golubitsky, *Nilpotent Hopf bifurcations in coupled cell systems*, SIAM J. Appl. Dynam. Sys., **5** (2006), 205–251.
- [4] J.-M. Gambaudo, *Perturbation of a Hopf bifurcation by an external time-periodic forcing*, J. Diff. Eqns., **57** (1985), 172–199.
- [5] M. Golubitsky, M. Nicol and I. Stewart, *Some curious phenomena in coupled cell networks*, J. Nonlinear Sci., **14** (2004), 207–236.
- [6] M. Golubitsky, C. Postlethwaite, L.-J. Shiau and Y. Zhang, *The feed-forward chain as a filter amplifier motif*, in “Coherent Behavior in Neuronal Networks,” (eds. K. Josic, M. Matias, R. Romo and J. Rubin), Springer Ser. Comput. Neurosci., **3**, Springer, New York, (2009), 95–120.
- [7] M. Golubitsky and D. G. Schaeffer, “Singularities and Groups in Bifurcation Theory,” Vol. I, Appl. Math. Sci., **51**, Springer-Verlag, New York, 1985.
- [8] M. Golubitsky, I. N. Stewart and D. G. Schaeffer, “Singularities and Groups in Bifurcation Theory,” Vol. II, Appl. Math. Sci., **69**, Springer-Verlag, New York, 1988.
- [9] N. J. McCullen, T. Mullin and M. Golubitsky, *Sensitive signal detection using a feed-forward oscillator network*, Phys. Rev. Lett., **98** (2007), 254101.
- [10] Y. Zhang, “Periodic Forcing of a System Near a Hopf Bifurcation Point,” Ph.D Thesis, Department of Mathematics, Ohio State University, 2010.

- [11] Y. Zhang and M. Golubitsky, *Periodically forced Hopf bifurcation*, SIAM J. Appl. Dynam. Sys., to appear.

Received June 2011; revised August 2011.

*E-mail address:* [mg@mbi.osu.edu](mailto:mg@mbi.osu.edu)

*E-mail address:* [c.postlethwaite@auckland.ac.nz](mailto:c.postlethwaite@auckland.ac.nz)